Macroalgae suspensions prepared by physical treatments: Effect of polysaccharide composition and microstructure on the rheological

Food Hydrocolloids xxx (xxxx) xxx

Contents lists available at ScienceDirect

Food Hydrocolloids

journal homepage: www.elsevier.com/locate/foodhyd

Macroalgae suspensions prepared by physical treatments: Effect of polysaccharide composition and microstructure on the rheological properties

Loredana Malafronte [a], Secil Yilmaz-Turan [b], Annika Krona [a], Marta Martinez-Sanz [c], Francisco Vilaplana [b], Patricia Lopez-Sanchez [a,d,*]

[a] Division of Bioeconomy and Health, Department Agriculture and Food, RISE Research Institutes of Sweden, Frans Perssons Väg 6, SE-41276, Gothenburg, Sweden
[b] Division of Glycoscience, Department of Chemistry, School of Engineering Sciences in Chemistry, Biotechnology and Health, KTH Royal Institute of Technology, AlbaNova University Centre, SE-106 91, Stockholm, Sweden
[c] Department of Food Safety and Preservation, IATA-CSIC, Avda. Agustin Escardino 7, 46980, Paterna, Valencia, Spain
[d] Division of Food and Nutrition Science, Biology and Biological Engineering, Chalmers University of Technology, SE-412 96, Gothenburg, Sweden

ARTICLE INFO

Keywords:
Algae
Polysaccharides
Suspensions
Rheology
Structure
High pressure homogenisation

ABSTRACT

The use of macroalgae in food products is growing due to their techno-functionality and nutritional properties. In this context, an increased understanding of the rheological properties which are relevant for manufacturing and texture is needed. Here we investigated the impact of thermal and mechanical treatments, including high pressure homogenisation (HPH), on the polysaccharide composition, microstructure, and rheological properties of brown algae *Laminaria digitata* suspensions (5 wt %). Monosaccharide analysis and immunolabeling of alginate in combination with confocal laser scanning microscopy, revealed a sequential release of different polysaccharides as result of the applied shear. Results showed that thermal treatment (70 °C 1 h) and mild shear lead to suspensions of clusters of cells and release of fucoidan and laminarin into the liquid phase, conferring shear thinning properties to the suspensions. High pressure homogenisation was able to completely break the macroalgae cells, reducing particle size and releasing other soluble polysaccharides, in particular alginate, conferring gel properties (G'>G'') to the suspensions. This study contributes to the knowledge of how to design sustainable, innovative and nutritious liquid/semiliquid food products containing macroalgae biomass.

1. Introduction

The transformation of the food chain is key for the achievement of the United Nations Sustainable Development Goals related to promote healthy diets and reduce environmental impact. By 2050 the world population is predicted to increase to almost 10 billion, which translates in an increased requirement of the food production of about 70% as compared to 2012. It is unlikely that this increase in production would be achieved using only land resources. There is a need to adopt emerging technologies like vertical agriculture, circular feeds for livestock and fish, insect-based foods/feed (Herrero et al., 2020) as well as to further investigate how to sustainably utilise ocean supplies. Among the food resources available in the oceans, marine macroalgae (seaweeds) have been identified as one of the 50 future foods that will contribute to transforming our global food system, based on their nutritional content, environmental impact, affordability, accessibility and acceptability (FAO et al., 2018; World Wildlife Foundation, Knorr Foods, & Adam Drewnowski, 2019).

Research on exploitation of seaweed biomass has been continuously growing in the last decades, because of their high content of economically important components such as polysaccharides, proteins, polyunsaturated fatty acids (PUFA) including omega-3 fatty acids, and antioxidants (Ścieszka & Klewicka, 2019), which are used in the chemical, pharmaceutical and food industries. Nowadays, the main interest of the food industry in seaweeds is as a source of polysaccharides such as alginate, carrageenan and agar, which are used as thickeners, gelling agents and to improve water absorption in food products i.e confectionery, dairy, desserts, bakery, meat and dressings (Wang, Chen,

* Corresponding author. Division of Food and Nutrition Science, Biology and Biological Engineering, Chalmers University of Technology, SE-412 96, Gothenburg, Sweden.
E-mail address: patlop@chalmers.se (P. Lopez-Sanchez).

https://doi.org/10.1016/j.foodhyd.2021.106989
Received 9 December 2020; Received in revised form 18 May 2021; Accepted 23 June 2021
Available online 25 June 2021

Huynh, & Chang, 2015; Ścieszka & Klewicka, 2019). Emerging innovative extraction technologies are being developed to maximise polysaccharides extraction yields (Gomez et al., 2020). An increased number of studies focuses on a biorefinery approach, starting from the whole seaweed and sequentially extracting the multiple high value compounds for different applications, including biofuels (Wei, Quarterman, & Jin, 2013). Taking this biorefinery approach, an enhancement of protein and bioethanol yields from *Laminaria digitata* was achieved by disrupting cell walls and hydrolysing cell wall polysaccharides (Hou, Hansen, & Bjerre, 2015); and agar extraction was combined with bioethanol production to optimise utilisation of *Gracilaria verrucosa* (Kumar, Gupta, Kumar, Sahoo, & Kuhad, 2013).

The use of seaweeds as food ingredients and the development of food products based on seaweeds are still challenging, due to the limited knowledge available on how to incorporate this biomass at an industrial scale. In addition, there are also challenges associated to the impact of seaweeds on the overall aspect and sensory properties of food products (Gupta & Abu-Ghannam, 2011), despite the positive attitude of western consumers towards their consumption (Lucas, Gouin, & Lesueur, 2019; Palmieri & Forleo, 2020; Wendin & Undeland, 2020). Studies showed that addition of seaweeds to meat and cereal based products can improve water and fat binding properties (Cofrades, López-López, Solas, Bravo, & Jiménez-Colmenero, 2008) as well as oxidative stability of meat products (López-López et al., 2009). Incorporation of seaweeds to pasta can improve its nutritional content of amino acids and fatty acids (Prabhasankar et al., 2009), whilst having a limited effect on the texture (Frafinho, Raymundo, Sousa, Dominguez, & Torres, 2019). Product development could benefit from more fundamental investigations on how algae could be utilised as a biomass source for food applications. In particular, the impact of food processing conditions on the seaweed microstructure and rheological properties of their suspensions, which are important for processability and product properties, would aid use of algae in foods.

High pressure homogenisation (HPH) is a high shear process (Schultz, Wagner, Urban, & Ulrich, 2004) commonly used to produce emulsions, and research has shown that it could be used to process plant materials and generate different textures (Bernaerts, Gheysen, Foubert, Hendrickx, & Van Loey, 2019; Lopez-Sanchez, Nijsse, et al., 2011). In the homogeniser, pressure is used to force a suspension through a small constriction and particles are disintegrated due to the different types of flows occurring, leading to the release of cell components i.e techno-functional ingredients and nutrients.

HPH has been previously used to disrupt plant tissues and impact the flow behaviour of fruits and vegetables suspensions (Lopez-Sanchez, Svelander, Bialek, Schumm, & Langton, 2011; Moelants et al., 2014; Zhou et al., 2017) including microalgae suspensions (Bernaerts 2019). However, to the best of our knowledge, no studies are available on the relationship between high pressure homogenisation/microstructure and rheological properties of macroalgae i.e seaweed. Therefore, the aim of this study was to investigate how high pressure homogenisation (HPH), in combination with thermal treatments, impacts the polysaccharide composition, microstructure and rheology of suspensions of the brown algae *Laminaria digitata*. Our results support the utilisation of macroalgae biomass as natural texturisers for food applications.

2. Materials and methods

2.1. Raw materials

Dried *Laminaria digitata* was purchased from KosterAlg (Swedish grower). The seaweed leaves were grown and dried under food grade conditions. The composition (expressed in dry weight as provided by the supplier) was total fat 0.68 wt %, total carbohydrate 55.8 wt%, total protein 9.12 wt% and total ash 25.4 wt%. The dried seaweed material was stored in a controlled temperature and humidity chamber at 14 °C and 30% RH prior to the experiments.

2.2. Preparation of algae suspensions

The preparation of the algae suspensions comprised the following steps. Dry algae leaves were first ground into flakes in a food processor (MCM 2054, Bosch, Germany) at speed 1 (ca. 1400 rpm) for 30s, and subsequently into powder in a coffee grinder (CEG 1.0, Andersson, Borås, Sweden) for 30s. A batch of 2L was prepared by combining algae powders with MilliQ water to a final solid content of 5 wt%. This batch suspension was divided in 250 mL sub-batches and left overnight in the fridge at 4 °C to allow the algae to rehydrate. Samples were separated in two sets and thermally treated at 70 °C or 90 °C for a total time of 1h. The temperatures were selected based on preliminary tests and as examples of mild (70 °C) and intense (90 °C) heating conditions. Temperature profiles during heating were recorded using a thermometer TESTO 735–2 (Testo AG; Germany). It took 10 min to reach 70 °C and about 30 min to reach 90 °C. After heating, the suspensions were quickly cooled down to room temperature using a cold-water bath followed by blending in a kitchen blender (5KSB553, KitchenAid Artisan, Michigan USA) for 60 s using the function puree, which corresponds to a speed of maximum 11,500 rpm as reported on the technical datasheet (mechanical treatment I). A subset of these samples were further mechanically treated using an ultraturrax (DI 25 basic, IKA-Werke GmbH & Co. KG, Germany) for 60 s at 13,500 rpm prior to high pressure homogenisation (GEA Niro Soavi, NS1001L2K, Italy) (mechanical treatment II). In the high pressure homogeniser the samples were treated using 2 stage homogenisation and 3 cycles with the following whole pressure (P1) to back pressure (P2) ratio: cycle 1 = 150/10 bar, cycle 2 = cycle 3 = 500/50 bar. The mechanical treatments I and II were performed on suspensions at room temperature and no variation in temperature was detected after HPH. The conditions for the mechanical treatments are based on preliminary trials aiming at a mild shear (mechanical treatment I) and an intense shear (mechanical treatment II) treatment. Pre-homogenisation with ultraturrax and 3 cycles of HPH were needed to achieve a high degree of cell breakage (supplementary Figure S1). An overview of the processing conditions is shown in supplementary Figure S2.

The liquid phase i.e supernatant and the dispersed phase i.e pellet, were separated after mechanical treatment I and II using a Heraus Megafuge 16R centrifuge (ThermoFisher Scientific, MA USA) equipped with a HIGHconic fixed angle rotor at 7000 rpm (6573 g), for 10 min at 25 °C. Approximately 20 mL of the suspensions before centrifugation and 20 mL of the liquid phase obtained after centrifugation were freeze-dried for subsequent chemical analysis.

The following annotation will be used throughout the text:

- T70-B: thermal treatment at 70 °C followed by blending (mechanical treatment I)
- T90-B: thermal treatment at 90 °C followed by blending (mechanical treatment I)
- T70-B-HPH: thermal treatment at 70 °C followed by blending, ultraturrax treatment and high pressure homogenisation (mechanical treatment II)
- T90-B-HPH: thermal treatment at 90 °C followed by blending, ultraturrax treatment and high pressure homogenisation (mechanical treatment II)

2.3. Monosaccharide analysis

The monosaccharide composition of the initial dried *Laminaria digitata*, the suspensions and the supernatants separated after centrifugation was determined after two-step methanolysis (Appeldoorn, Kabel, Van Eylen, Gruppen, & Schols, 2010; Martínez-Abad, Giummarella, Lawoko, & Vilaplana, 2018). Briefly, 1 mg of dry sample was hydrolysed using 1 mL of 2 M HCl in dry methanol at 100 °C for 5 h. Samples were then neutralised with pyridine followed by drying under air. Further hydrolysis was carried out using 2 M trifluoro acetic acid (TFA) at 120 °C

for 1 h. Samples were dried again under air, redissolved in water and injected onto a high-performance anion exchange chromatographer with pulsed amperometric detection (HPAEC-PAD) system (Dionex ICS 3000, Sunnyvale, CA, USA) equipped with a CarboPac PA1 column (4 × 250 mm, Dionex). The eluent program was applied as described by McKee et al. (2016). Neutral and uronic sugar standards at concentrations between 0.005 and 0.1 g/L were used for the quantification of monosaccharides. The experiments were performed in triplicate.

2.4. Soluble protein content

The soluble protein content was determined using the dye-binding Bradford assay (Bradford, 1976). Briefly, 10 mg/mL aqueous solution of sample was mixed with the dye reagent (1:50 v/v) and incubated at room temperature for 15 min. The absorbance of the samples was then measured at 595 nm using a UV–Vis spectrophotometer (Varian Cary 50 UV-VIS, Agilent) and the protein content was calculated using the standard calibration of bovine serum albumin. The measurements were done in triplicate.

2.5. Molar mass distribution

The molar mass distributions of the algae suspensions were analysed using size exclusion chromatography (SEC) coupled to a refractive index detector (SECcurity 1260, Polymer Standard Services, Mainz, Germany). Separation was achieved using a column set consisting of a GRAM PreColumn, 30 and 10,000 analytical columns (Polymer Standard Services, Mainz, Germany) with a flow rate of 0.5 mL/min at 60 °C. Prior to SEC analysis, the samples were dissolved in DMSO supplemented with 0.5% (w/v) LiBr at 60 °C overnight with concentration of 3 mg/mL and filtered through a 0.2 μm Nylon filter to remove any undispersed particulates. Standard calibration was performed using pullulan standards between 342 and 708,000 Da (Polymer Standard Services, Mainz, Germany).

2.6. Particle size distribution

Particle size distribution of the suspensions was determined using a laser diffraction particle size analyzer, Malvern Mastersizer 3000 equipped with a Hydro MV accessory for liquid samples (Malvern Instruments, UK). The measurements were performed using MilliQ water at 25 °C as dispersant. The specific surface area and particle size, in terms of surface weighted mean, D [3,2], and volume weighted mean, D [4,3], were determined using a refractive index of 1.4683 and an absorption index of 0.01.

2.7. Light microscopy

Algae suspensions were frozen in molds in liquid nitrogen and freeze sectioned in a Leica CM1900 cryostat, stained with Lugol's solution and analysed in an Olympus BX53 light microscope (Olympus Corporation, Tokyo, Japan). Digital images were taken using an CMos camera SC50 (Olympus). Acquired images were analysed and processed using Olympus cellSense Entry.

2.8. Immuno-labelling and confocal laser scanning microscopy (CLSM)

Cryo-sections of *Laminaria digitata* suspensions were fixated for 30 min in 4% paraformaldehyde in phosphate-buffered saline (PBS) buffer (pH 7.4) and rinsed with PBS. The sections were then pre-incubated for 40 min in PBS buffer with 2.5% BSA before applying the primary antibody to label alginate BAM10 (Plant Probes, Leeds, UK) diluted 1:50 in PBS containing 0.5% BSA, for 2 h. After incubation, the sections were rinsed thoroughly with PBS and then incubated for 2 h in the dark with fluorescently labelled secondary antibody Alexa Fluor® 488 (Invitrogen, Carlsbad, CA, USA). All incubations were performed in moisturised chambers at room temperature. Sections were then rinsed with PBS and water and mounted with ProLong®Diamond (Invitrogen, Carlsbad, CA, USA) anti-fading reagent. Micrographs were acquired using a CLSM (Leica TCS SP5, Heidelberg, Germany) with a HCX PL APO lambda blue 20.0x0.70 IMM UV objective, zoom 1× and 3x. A 488 nm Ar laser and a 633 nm HeNe laser were used for excitation. Emissions were collected at 500–540 for alginate (green) and 645–715 nm for autofluorescence from chlorophyll (red). Image format 1024x1024 pixels, 8 lines average. Autofluorescence of cell walls (green) were analysed using the same settings on unstained samples mounted in ProLong®Diamond (Invitrogen, Carlsbad, CA, USA) anti-fading reagent.

2.9. Shear viscosity and viscoelasticity

The suspensions were degassed under vacuum prior to rheological characterisation. The shear viscosity (η_s) and the viscoelastic moduli were measured using a strain-controlled rheometer ARES-G2 (TA Instrument, DE, USA), equipped with a parallel-plate geometry with a diameter of 40 mm. Measurements were performed at 25 °C and 1 mm gap. A solvent trap was used to prevent evaporation during the measurements. Shear viscosity was measured at increasing shear rate from 1 to 100 s^{-1}. Viscoelasticity was evaluated in the linear region, which was determined by applying a strain sweep from 0.1 to 100% at a constant frequency of 1 Hz. A frequency sweep from 0.1 to 20 Hz at 1% strain was used to obtained viscoelastic moduli. The viscoelasticity results are shown in terms of storage modulus(G′) and loss modulus (G′′). Samples were measured in duplicates.

2.10. Extensional viscosity

Extensional viscosity (η_E) was determined using a Hyperbolic Contraction Flow (HCF) geometry mounted in an Instron 5542 (Instron Corp., Canton). Details of the method are described in previous publications (Stading & Bohlin, 2001; Wikström & Bohlin, 1999). The HCF method forces a fluid through a hyperbolic contraction nozzle to extend it to a maximum Hencky strain (ε_H) given by the specific nozzle and the shear thinning index of the fluid. The resulting stress on the nozzle is monitored through the force recorded on the Instron instrument. During contraction flow the fluid experiences extension and shear, the shear contribution was subtracted from the total measured stress by calculating the shear contribution as a function of the shear thinning index (n) and the flow consistence index (k). The parameters n and k were obtained from the shear viscosity measurements assuming a power-law:

$$\sigma_{shear} = k\dot{\gamma}^n \quad (1)$$

where σ_{shear} is the shear stress and $\dot{\gamma}$ the shear rate.

A 10N load cell and a nozzle with the following dimensions: height = 15 mm, inlet radius = 10 mm and outlet radius = 0,83 mm were used. Before measurements, all samples were conditioned at 25 °C for at least 2h in a water bath. The measurements were performed at 25 °C controlled by a water jacket. Extension rates ranging from 7 to 150 s^{-1} were investigated. Measurements were performed in triplicates.

The Trouton ratio (T_r) was calculated at an extensional rate ($\dot{\varepsilon}$) equal to the shear rate ($\dot{\gamma}$) using the following equation:

$$T_r = \frac{\eta_E(\dot{\varepsilon})}{\eta_s(\dot{\gamma})} \quad (2)$$

where η_E is the extensional viscosity and η_S is the shear viscosity.

3. Results and discussion

3.1. Carbohydrate content as result of thermal and mechanical treatments

The measured carbohydrate content represented approximately 41 wt% of the total composition. The monosaccharide composition of the

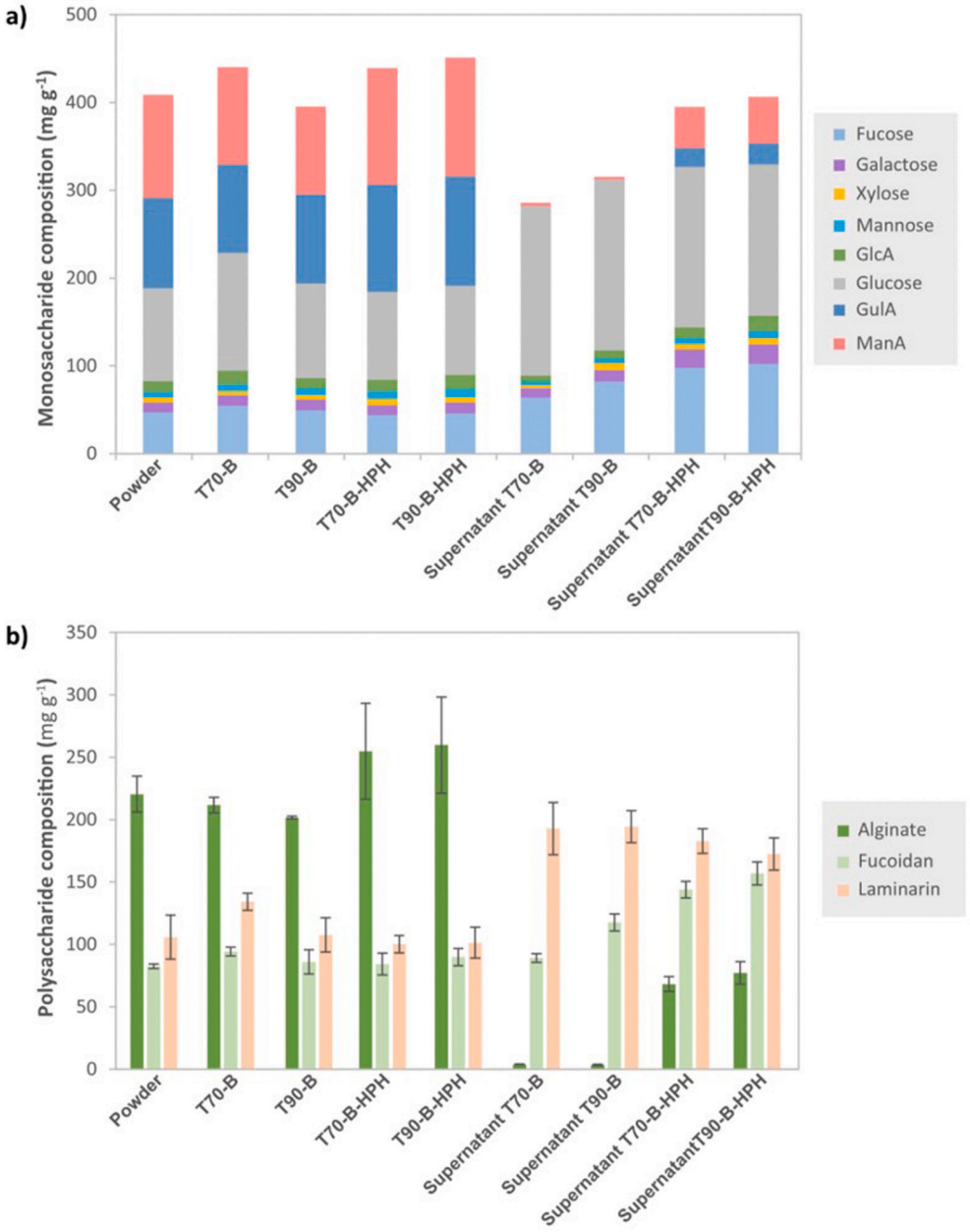

Fig. 1. Monosaccharide (a) and polysaccharide (b) content of *Laminaria digitata* dry powder, suspensions and corresponding supernatants expressed in dry weight bases. Glc = glucose; GulA = guluronic acid; GlcA = glucuronic acid; ManA = mannuronic acid. Arabinose, rhamnose and galacturonic acid were not detected. T70-B: thermal treatment at 70 °C followed by blending, T90-B: thermal treatment at 90 °C followed by blending, T70-B-HPH: thermal treatment at 70 °C followed by blending, ultraturrax treatment and high pressure homogenisation and T90-B-HPH: thermal treatment at 90 °C followed by blending, ultraturrax treatment and high pressure homogenisation.

samples is shown in Fig. 1a. The monosaccharide analysis demonstrated that the major component in the initial *L. digitata* powder were uronic acids (mannuronic acid (ManA) and guluronic acid (GulA)) and glucose (Glc). The total of ManA and GulA accounted for 22% (dry weight) of the biomass and was attributed to alginate, which is usually present in the cell wall at a concentration between 25 and 40% of the dry weight (Qin, 2008). Glc, on the other hand, comprised approximately 11% of the initial algae and mostly originated from laminarin ((1-3-)-β-D-glucan) (Zvyagintseva et al., 1999). Laminarin is one of the main carbon storages in seaweed ranging from 1 to 25% (Adams, Toop, Donnison, & Gallagher, 2011). Fucose (Fuc) and galactose (Gal) were ascribed to fucoidan with branches of xylose (Xyl), mannose (Man) and glucuronic acid (GlcA) (Li, Lu, Wei, & Zhao, 2008), which represented nearly 8% of the total sample and with the role to protect the seaweeds from desiccation (Anastasakis, Ross, & Jones, 2011).The monosaccharide composition of *L. digitata* is in agreement with previous studies (Allahgholi et al., 2020).

The suspensions and the corresponding supernatants were analysed. It is worth noting that supernatant separation was difficult in high pressure homogenised samples, before HPH about 70 wt % supernatant was separated (mechanical treatment I), instead for the high pressure homogenised (HPH) suspensions only 20 wt % supernatant was obtained (mechanical treatment II). This is likely due to the increased viscosity and viscoelasticity of HPH samples, as it will be shown and discussed later on in the text, increasing the difficulty to separate the liquid phase. The suspensions before HPH (T70-B and T90-B) exhibited a slightly lower uronic acid content compared to the initial *L. digitata* powder, whereas suspensions after HPH (T70-B-HPH and T90-B-HPH) contained higher amounts of both ManA and GulA. This suggested that the HPH treatment enriched the alginate content of the suspensions at both 70 °C and 90 °C. The glucose content of the suspensions was higher before HPH as compared to the suspensions after HPH, implying a higher laminarin composition before HPH. Likewise, the fucoidan content (Fuc + Gal + Xyl + Man + GlcA) of the suspensions decreased after HPH. There were not significant differences between the monosaccharide composition of the suspensions at 90 °C and 70 °C (Fig. 1b).

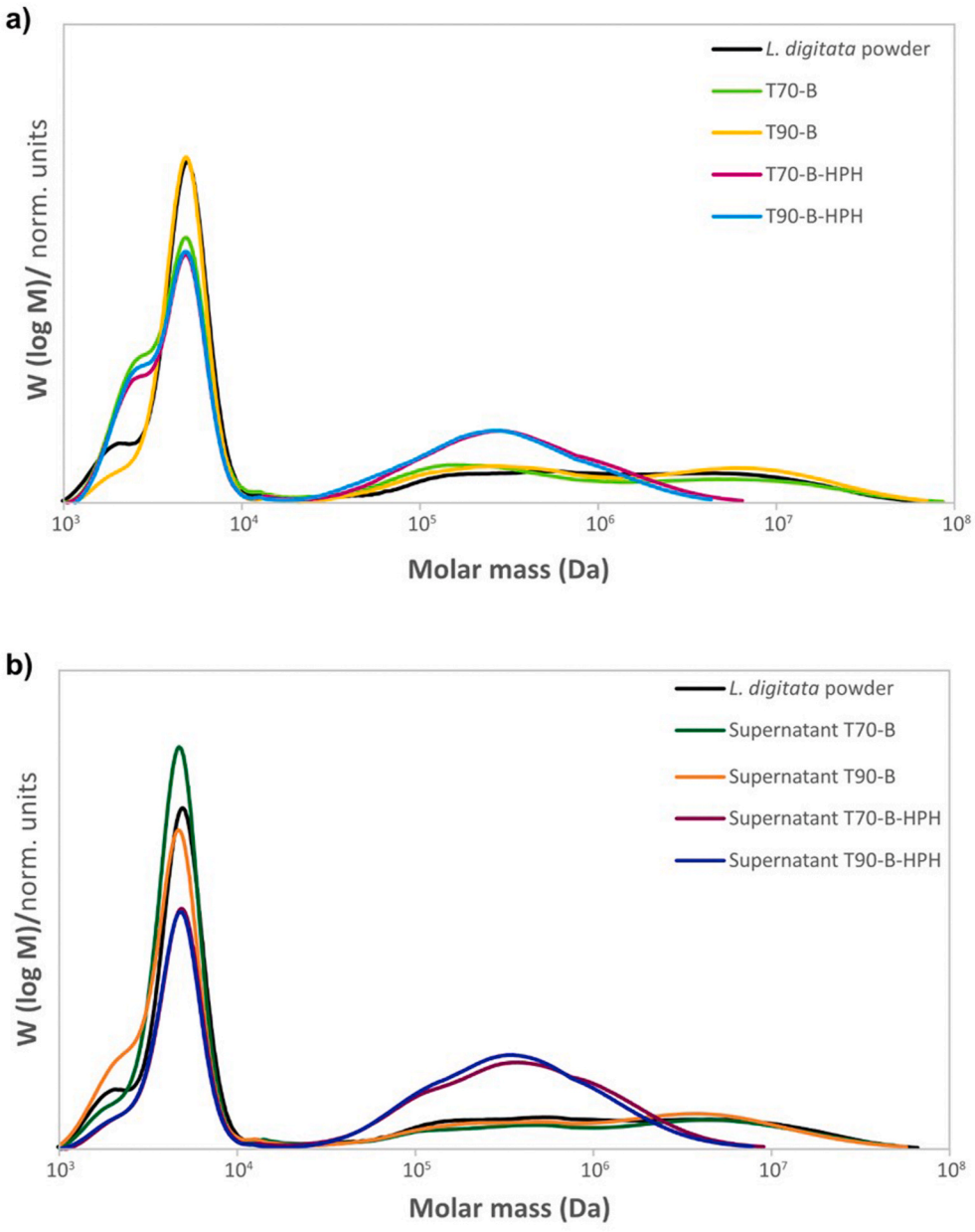

Fig. 2. Molar mass distributions of (a) *Laminaria digitata* suspensions and (b) supernatants after different thermal and mechanical treatments. T70-B: thermal treatment at 70 °C followed by blending, T90-B: thermal treatment at 90 °C followed by blending, T70-B-HPH: thermal treatment at 70 °C followed by blending, ultraturrax treatment and high pressure homogenisation and T90-B-HPH: thermal treatment at 90 °C followed by blending, ultraturrax treatment and high pressure homogenisation.

As for the monosaccharide composition of the supernatants (Fig. 1a), higher contents of Fuc, Gal and Glc, and much lower ManA and GulA were observed in all supernatants compared to the suspensions. This indicated that fucoidan and laminarin were solubilised and recovered in the supernatants after both mechanical treatments. Comparing the supernatants, Glc was the dominating sugar in the supernatant before HPH, whereas Fuc and uronic acids (GlcA, GulA and ManA) were the main sugars after HPH. This demonstrated that the prominent polysaccharides in the supernatants changed from laminarin and fucoidan to alginate (Fig. 1b). The high fucoidan content of the supernatants, together with laminarin, became more pronounced after HPH, indicating that the combination of blending, ultraturrax and high pressure homogenisation (mechanical treatment II) is more effective than only blending (mechanical treatment I) to solubilise different polysaccharides. Regarding the effect of the two temperatures on the supernatants, a general increase was observed in the content of all monosaccharides at 90 °C after both treatments. This was attributed to the higher efficiency of the high temperature to extract carbohydrates (Ruthes, Martínez-Abad, Tan, Bulone, & Vilaplana, 2017; Saravana, Cho, Woo, & Chun, 2018) as the total carbohydrate yield also generally increased after all treatments at 90 °C (both for suspensions and supernatants).

3.2. Impact of processing on the molar mass distributions

The SEC chromatograms of the algae suspensions and supernatants are shown in Fig. 2, and the relative number- (Mn) and weight-average (Mw) molecular weights obtained from calibration with pullulan standards are presented in Table 1. The SEC analysis demonstrated a wide range of relative molar mass distributions and two main populations corresponding to a mixture of low (L) and high (H) molar mass components of the samples. The low and high molar mass populations of the initial *L. digitata* biomass were centered at 5 kDa and 1400 kDa, respectively. The low molar mass populations likely corresponded to laminarin (Graiff, Ruth, Kragl, & Karsten, 2016) and the high molar mass fractions can be attributed mainly to fucoidan and alginate (Flórez-Fernández, Torres, González-Muñoz, & Domínguez, 2018). The SEC analysis of the suspensions and supernatants before and after HPH

Table 1
Number- and weight-average molar mass of low (L) and high (H) molar mass fractions of initial powder, the suspensions and corresponding supernatants. T70-B: thermal treatment at 70 °C followed by blending, T90-B: thermal treatment at 90 °C followed by blending, T70-B-HPH: thermal treatment at 70 °C followed by blending, ultraturrax treatment and high pressure homogenisation and T90-B-HPH: thermal treatment at 90 °C followed by blending, ultraturrax treatment and high pressure homogenisation.

		M_n (kDa)	M_w (kDa)
Powder	L	4.49	4.95
	H	1467.00	1471.00
T70-B	L	3.51	4.34
	H	786.00	869.70
T90-B	L	4.17	4.73
	H	316.60	5304.00
T70-B-HPH	L	3.47	4.18
	H	194.20	621.30
T90-B-HPH	L	3.49	4.17
	H	167.10	512.00
Supernatant T70-B	L	3.98	4.68
	H	3547.00	8867.00
Supernatant T90-B	L	3.48	4.22
	H	380.00	4581.00
Supernatant T70-B-HPH	L	4.08	4.70
	H	205.90	777.00
Supernatant T90-B-HPH	L	4.62	5.00
	H	185.20	620.70

treatment confirmed the presence of different components (i.e. alginate, fucoidan and laminarin) as observed by the monosaccharide analysis. The molar mass distributions of the suspensions before HPH (T70-B and T90-B) were very broad and similar to each other, regardless of the temperature applied, which indicate that the thermal treatment did not induce degradation of the polymeric components. Interestingly, the high molar mass fractions became monomodal after HPH (T70-B-HPH and T90-B-HPH, mechanical treatement II), confirming the enrichment of alginate by HPH as observed by the monosaccharide analysis. In all the suspensions a small shoulder was observed at 2.5 kDa, which could be attributed to oligomeric alginate (Nguyen et al., 2020).

As for the supernatants before HPH (supernatant T70-B and supernatant T90-B), the size distribution of the low molar mass populations was similar to those of the suspensions at both temperatures. The small shoulder observed in the suspensions at 2.5 kDa became much less apparent in all the supernatants, suggesting that oligomeric alginate was not recovered in the supernatants. The high molar mass populations, on the other hand, shifted towards higher molecular weight at both 70 °C and 90 °C. This corresponded to significantly decreased content of alginate, making the fucoidan the major polysaccharide in these fractions (Fig. 1b). The supernatants after HPH, exhibited a monomodal size distribution of the high molar mass populations corresponding to higher alginate and fucoidan content of these fractions. The molar mass distributions after HPH treatment shifted to lower values, which could be attributed to the degradation of the very large polysaccharide chains, the dissociation of the large polysaccharide aggregates or, to the low volume of supernatant recovered from HPH samples after centrifugation. As mentioned previously, after HPH it was difficult to separate the liquid phase due to the increased viscosity and viscoelasticity of HPH samples. Smaller molecules are expected to be easier to separate with the centrifugation conditions used. Concerning the effect of temperature on the molar mass distribution, processing at 90 °C caused a general

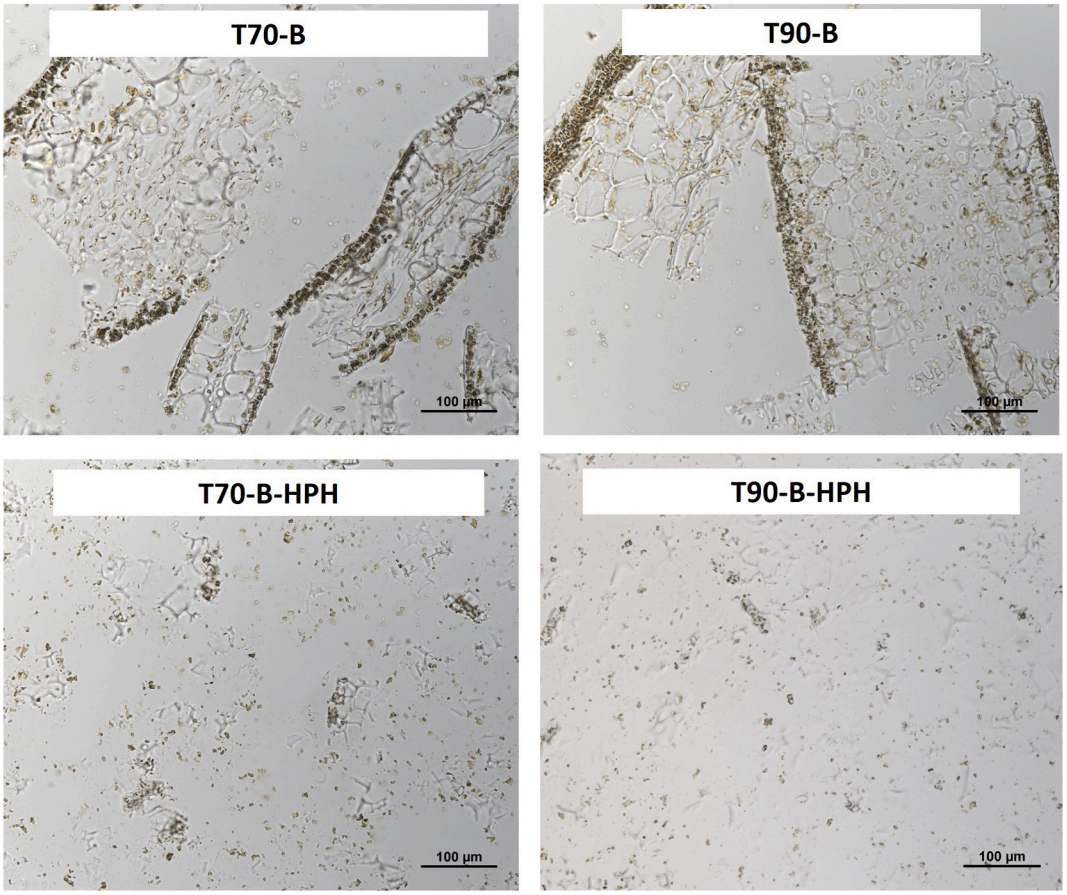

Fig. 3. Light microscopy images of suspensions of *Laminaria digitata* (5 wt%). Top row represents the suspensions processed at 70 °C and 90 °C before high pressure homogenisation (T70-B and T90-B). Bottom row represents the suspensions after high pressure homogenisation (T70-B-HPH and T90-B-HPH). Samples were stained with Lugol's solution to get better contrast between different cell components by staining proteins brown/yellow. Cell walls are unstained, and chloroplasts are green.

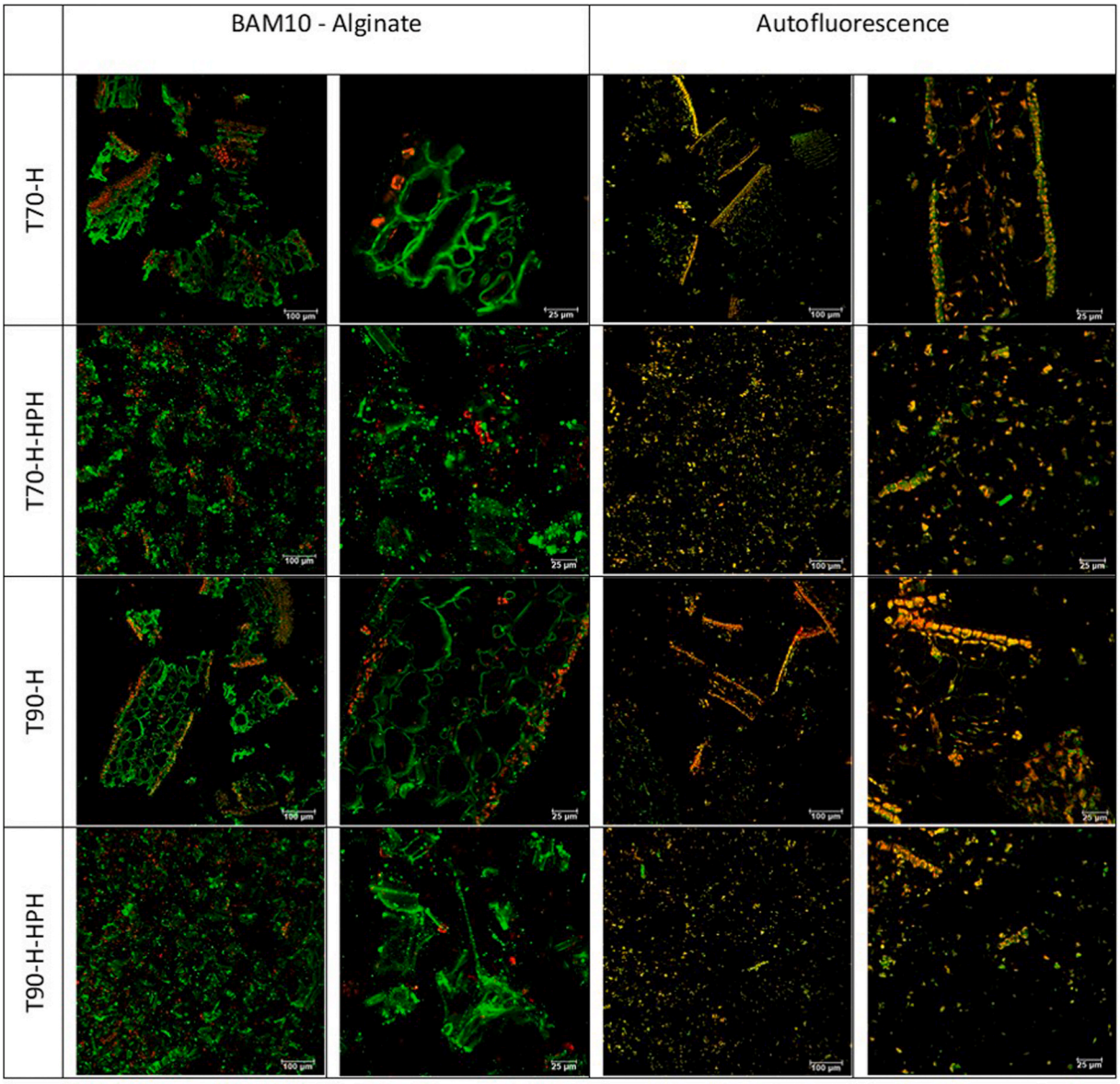

Fig. 4. Confocal scanning laser microscopy images of suspensions of *Laminaria digitata* (5 wt%). Samples were immunolabeled for alginate with BAM10, shown in green (left). Autofluorescence from cell walls was evaluated in unstained samples, shown in green (right). Red signal comes from autofluorescence in chloroplasts. Images represent suspensions processed at 70 °C and 90 °C before high pressure homogenisation (T70-B and T90-B, mechanical treatment I) and after high pressure homogenisation (T70-B-HPH and T90-B-HPH, mechanical treatment II). Two different magnifications are shown for each sample. (For interpretation of the references to colour in this figure legend, the reader is referred to the Web version of this article.)

decrease in the molar mass of all suspensions and supernatants as compared to 70 °C. This was related to the hydrolysing effect of high temperature on polysaccharides in accordance with previous studies (Yilmaz-Turan et al., 2020).

3.3. Impact of high pressure homogenisation on soluble protein content

The total protein content in the *Laminaria digitata* powder was 9.1 wt % (measured by Kjeldahl method and in agreement with supplier specifications) and the soluble protein was not detected. *L. digitata* has been reported to contain 5-7 wt % proteins, glutamic acid and aspartic acid are the two most abundant amino acids, (Schiener, Black, Stanley, & Green, 2014). The small difference between previously reported values and ours is expected for biological materials, and could be due to the use of different materials (harvest time, part of the plant) and methodology. Both mechanical treatments released a small amount of soluble proteins in the supernatants, 0.37 ± 0.02 wt% and 0.41 ± 0.01 wt% for 70 °C and 90 °C respectively and slightly higher after HPH, 0.55 ± 0.06 wt% and 0.57 ± 0.01 wt % for 70 °C and 90 °C respectively. These values are very low compared to the total protein content, it has been reported that the extraction of proteins from brown seaweeds could be hindered by their strong interaction with polysaccharides and polyphenols (Abdollahi et al., 2019). For the HPH supernatant a higher protein content was expected, due to the high degree of cell damage achieved (Fig. 3) however, the low soluble protein content detected in the HPH supernatant could be also affected by the high viscosity of the suspensions (subsection 3.5), which made it difficult to separate the supernatant by centrifugation.

3.4. Impact of processing on microstructure and particle size distribution

Light microscopy and confocal laser scanning microscopy (CLSM) revealed the degree of disruption of the macroalgae as result of thermal and mechanical treatments (Figs. 3 and 5). Particles in T70-B and T90-B

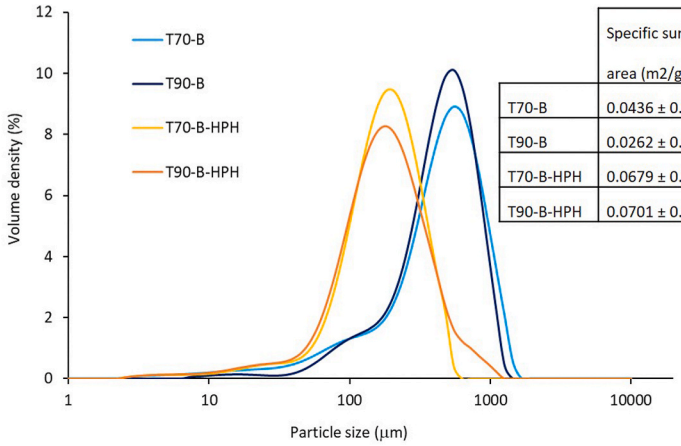

	Specific surface area (m2/g)	D [3,2] (µm)	D [4,3] (µm)	Uniformity
T70-B	0.0436 ± 0.0026	137.5 ± 8.3	463.2 ± 21.4	0.530
T90-B	0.0262 ± 0.0006	228.6 ± 5.0	445.1 ± 14.8	0.456
T70-B-HPH	0.0679 ± 0.0006	88.4 ± 0.8	181.3 ± 1.9	0.477
T90-B-HPH	0.0701 ± 0.0143	85.6 ± 20.0	199.8 ± 68.0	0.631

Fig. 5. Particle size distribution of *Laminaria digitata* suspensions (5 wt%) processed at 70 °C and 90 °C before high pressure homogenisation (T70-B and T90-B) and after high pressure homogenisation (T70-B-HPH and T90-B-HPH). Specific surface area and particle size determined from the DLS measurements (D [3,2]: surface weighted mean; D [4,3]: volume weighted mean). Average and standard deviation of three measurements.

suspensions were mainly comminuted blades, in which the hierarchical structure from epidermis to pith could be observed, and a few cell clusters without the outmost cell layers. *Laminaria digitata* is characterised by a stipe connected to a holdfast from which the blades branch out (Shi et al., 2011). At a microscopic level, the blades are composed of three basic structures, the epidermis, the dermal tissue and the pith. The epidermis is the outermost tissue consisting of small epidermal cells. The dermal, right below the epidermis, consists of an exodermis and an endoderm layer. The exodermis is a layer of cells smaller than the epidermis, the endoderm is a layer of cells larger than the exodermis and the pith is composed of cells remarkably smaller than the endoderm.

After high pressure homogenisation (samples T70-B-HPH and T90-B-HPH), the suspended particles were mainly cell fragments and few small clusters of damaged cells. The production of cell fragments using high pressure homogenisation has been previously shown for fruits and vegetables such as carrot and broccoli (Lopez-Sanchez, Nijsse, et al., 2011), mango (Zhou et al., 2017) and for microalgae (Bernaerts et al., 2019). Cell components could be visualised in the liquid phase after all treatments, especially after HPH. CLSM (Fig. 4) agreed well with light microscopy findings. Although samples were unstained the use of different autofluorescence wavelengths allowed visualisation of cell walls (in green) and chloroplasts (in red). The immunostaining of the suspensions with BAM10, which recognises guluronate-specific epitopes in alginate, showed that before HPH alginate was present preferably in the middle lamella, between intact cells (in green in Fig. 4). After HPH small droplets with strong fluorescence were seen in the suspensions (Fig. 4). This indicated that the alginate was released from the cell walls into the liquid phase, in accordance with the results from monosaccharide analysis (Fig. 1a). Since plant material could present autofluorescence in the same wavelength region that the antibody Alexa Fluor® 488 unstained samples were also examined as controls. Although, some autofluorescence was observed from cell walls, the pattern and signal strength were different than for the immuno-stained samples, confirming that alginate could be clearly identified.

Particle size distributions and specific surface area, surface weighted mean, D [3,2],volume weighted mean, D [4,3], and uniformity are represented in Fig. 5. All the suspensions showed narrow size distributions, indicating that the samples were quite homogeneous. The uniformity parameter was ca. 0.5 for all the samples, except for T90-B-HPH, which showed a slightly larger value of ca. 0.6, suggesting a greater heterogeneity in the measured particle sizes for this sample. The suspensions T70-B and T90-B showed a larger particle size and lower specific surface area than T70-B-HPH and T90-B-HPH. There were not significant differences in particle size as function of temperature (Fig. 5). The severity of the applied mechanical treatment did impact the cell size and morphology, after blending (mechanical treatment I) the D [4,3] was 463 µm and 445 µm for the 70 °C and 90 °C treatments respectively, whilst after high pressure homogenisation (mechanical treatment II) the size was reduced to 181 µm and 200 µm for 70 °C and 90 °C respectively.

The results from microscopy and particle size analysis indicated that particle microstructure depended mainly on the mechanical treatment and not on the thermal treatment. These results showed that increase temperature (70 °C–90 °C) did not change neither particle size nor morphology.

3.5. Effect of high pressure homogenisation on the rheological properties

The rheological properties of a suspension depend on the soluble components in the liquid phase and the particle volume fraction (Macosko, 1994). Particle parameters such as size, morphology, hardness, and inter-particle forces determine the effective particle volume fraction. The intense shear input of high pressure homogenisation (mechanical treatment II) led to an increase in cell disruption (Figs. 3 and 4) compared to blending (mechanical treatment I) and changed particle size, morphology and chemical composition of the liquid phase (Fig. 1) impacting the rheological properties (Fig. 6).

Before high pressure homogenisation, there was a clear difference in the stability of the suspensions. Indeed, T90-B could not be measured due to fast sedimentation, whilst T70-B was stable and showed shear thinning behaviour i.e the shear viscosity decreased with shear rate (Fig. 6a). The shear viscosity ranged from 0.63 Pa s to 0.08 Pa s in the range of shear rate investigated (1-100 s^{-1}). In this case, the differences observed between both suspensions could be explained based on the liquid phase properties. Although both supernatants had similar total solids content of 2.73 ± 0.04 wt % and 2.63 ± 0.01 wt % for 70 °C and 90 °C respectively, the supernatant in T90-B had low molar mass (Table 1), low viscosity (~0.02 Pa s) and showed Newtonian behaviour; whereas the supernatant in T70-B had higher molar mass polysaccharides (Table 1) leading to higher viscosity than supernatant T90-B and shear thinning behaviour. After high pressure homogenisation, the suspensions (T70-B-HPH and T90-B-HPH) had higher shear viscosity and exhibited shear thinning behaviour. They showed similar viscosity independently of the temperature, ranging from 15.96 Pa s to 0.93 Pa s in the range of shear rate investigated (1-100 s^{-1}), significantly higher than before high pressure homogenisation. In Table 2 the flow consistency index, k, and the shear thinning index, n, are reported. These constants were obtained from a power law fit of data in Fig. 6a. High k values indicate higher consistency, and low n values indicate a more pronounced shear-thinning behaviour, thus after high pressure homogenisation suspension had a higher consistency, k = 19 for T70-B-HPH

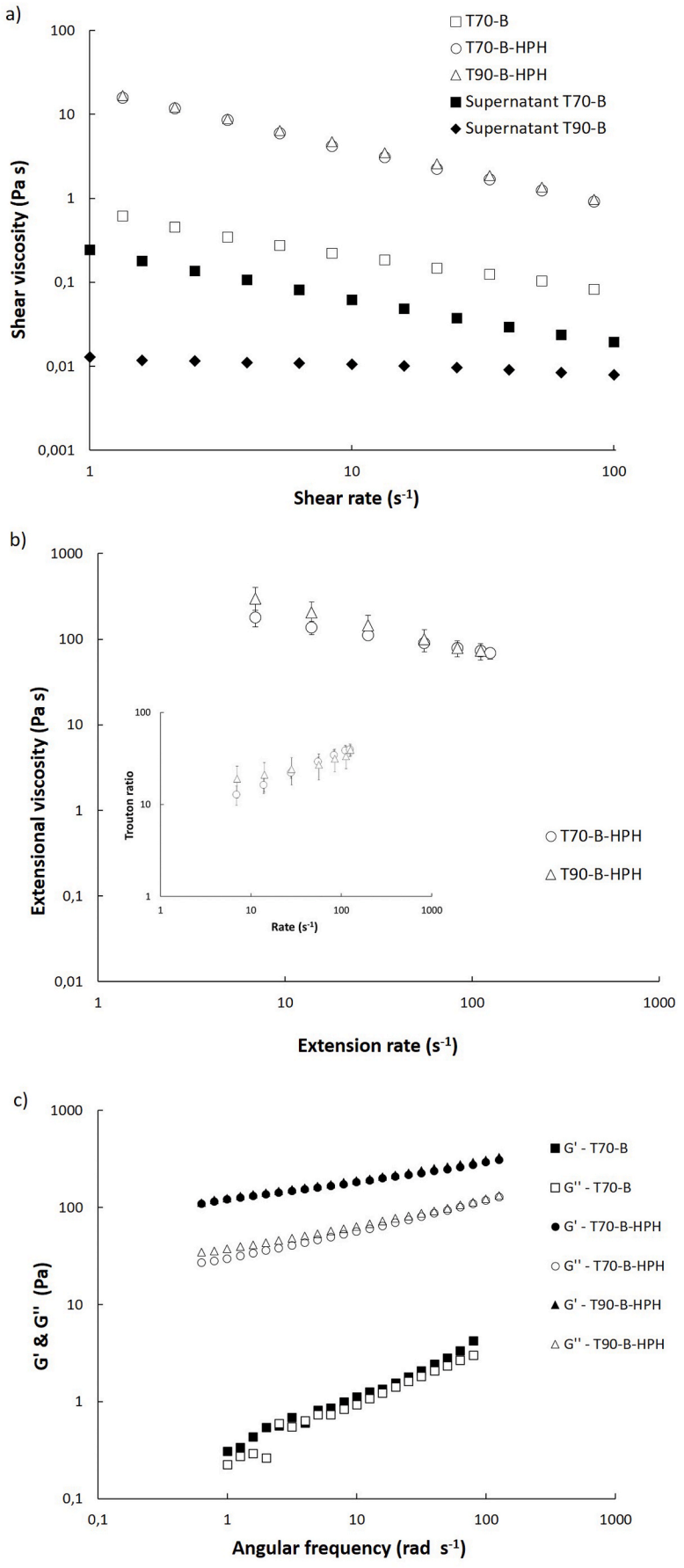

Fig. 6. (a) Representative shear viscosity curves of *Laminaria digitata* suspension (5 wt%) processed at 70 °C before high pressure homogenisation (T70-B) and after high pressure homogenisation (T70-B-HPH). Suspension processed at 90 °C after high pressure homogenisation (T90-B-HPH). Suspension T90-B sedimented and it was not possible to measure it. (b) Extensional viscosity of the suspensions after high pressure homogenisation. Before HPH suspensions had large particles and it was not possible to measure their extensional viscosity. The inset represents the Trouton value of the suspensions. (c) Representative elastic modulus G′ and viscous modulus G′′ of suspensions before and after high pressure homogenisation.

Table 2
Parameters obtained from Power law fitting of the shear stress vs shear rate data. n represents the flow index and k consistency. Average and standard deviation of 3 measurements are shown. Nm = not measured. *Laminaria digitata* suspension (5 wt%) processed at 70 °C before high pressure homogenisation (T70-B) and after high pressure homogenisation (T70-B-HPH). Suspension processed at 90 °C after high pressure homogenisation (T90-B-HPH). Suspension T90-B sedimented and it was not possible to measure it.

	n	k	ε_H
T70-B	0.54 ± 0.02	0.62 ± 0.02	Nm
T70-B-HPH	0.3 ± 0.01	19.21 ± 1.21	7.27
T90-B-HPH	0.33 ± 0.01	19.19 ± 2.03	7.27
Supernatant T70-B	0.44 ± 0.02	0.24 ± 0.01	Nm
Supernanant T90-B	0.93 ± 0.07	0.01 ± 0.00	Nm

and T90-B-HPH, and they were more shear thinning, n = 0.3, than prior to high pressure homogenisation n = 0.5. The release of alginate to the liquid phase and the changes in the particle properties (i.e smaller particles with higher surface area) could enhance particle-alginate interactions and particle– particle interactions explaining the higher consistency and shear thinning behaviour after high pressure homogenisation (mechanical treatment II).

The suspensions after high pressure homogenisation presented an apparent extensional viscosity (Fig. 6b), with similar values independently of the temperature, i.e 200 Pa s at an extensional rate of 10 s^{-1}. The extensional viscosity decreased with increasing extensional rate, showing an extension thinning behaviour. The presence of large particles that lodged in the instrument nozzle, led to unreliable measurements for suspensions before HPH. Furthermore, the extensional viscosity of the supernatants before HPH could not be accurately measured because it was lower than 10 Pa s, which is the threshold of the set up used in this study. The Trouton ratio of the suspensions after high pressure homogenisation was 20–40 from low to high shear/extensional rate (inset in Fig. 6b). The Trouton ratio of the suspensions T70-B-HPH and T90-B-HPH was higher than 10, above the Newtonian limit of Tr = 3, indicating that noticeable elastic contribution could be detected. The Hencky strains ε_H calculated from extensional viscosity (Table 2) was similar, indicating that they were subjected to a similar deformation.

The effect of high pressure homogenisation was also evaluated on the viscoelastic properties of the suspensions (Fig. 6c). Before HPH, samples behaved as particle suspensions with high frequency dependence. After HPH, both suspensions displayed a weak gel behaviour, with G'>G'' and slight frequency dependence. Fitting of G' vs angular frequency (ω) to power law model ($G' = a\,\omega^b$) shows that the G′ frequency dependency, which is given by the fitting parameter b, of T70-B (a = 0.31, b = 0.58, $R^2 = 0.98$) is higher than T70-B-HPH (a = 119.12, b = 0.19, $R^2 = 1$) and T90-B-HBH (a = 123.32, b = 0.19, $R^2 = 1$). This indicates that the latter two are more elastic (solid like) than T70-B. The changes in viscoelastic properties agrees well with chemical changes (Fig. 1) in which an increase in soluble polymers, specially the alginate extracted to the liquid phase, could lead to enhanced particle-liquid phase interactions and increased viscoelasticity. Soluble polysaccharides can increase the viscosity of the liquid phase thanks to their ability to expand, leading to higher hydrodynamic volumes when interacting with water. In certain cases, they can create gels by associative interactions between polysaccharides that lead to the formation of continuous networks able to hold water (Lovegrove et al., 2017).

4. Conclusions

Exploitation of macroalgae biomass is needed to meet future food consumption demands. A combination of thermal (70 °C 1h) with mild mechanical treatments, disrupted algae into cell clusters of different sizes and released polysaccharides in the liquid phase, mainly β-glucan laminarin, leading to stable shear-thinning suspensions with low viscosity (<1 Pa s). High pressure homogenisation (150–500 bar) disintegrated the cells completely, leading to cell fragments suspended in an alginate rich liquid phase increasing the viscosity more than tenfold and conferring gel properties to the suspensions. Suspensions prepared with whole *Laminaria digitata* could be utilised as structuring agents in food systems.

Author contributions

Loredana Malafronte: Conceptualization, Investigation, Formal analysis, Data curation Visualisation, Writing – original draft, Writing – review & editing. Secil Yilmaz-Turan: Investigation, Formal analysis, Visualisation, Data curation, Writing – original draft. Writing – review & editing. Annika Krona: Investigation, Formal analysis, Visualisation, Writing – original draft. Writing – review & editing. Marta Martinez-Sanz: Investigation, Formal analysis, Visualisation, Writing – original draft. Writing – review & editing. Francisco Vilaplana: Formal analysis, Writing – review & editing. Funding acquisition. Patricia Lopez-Sanchez: Conceptualization, Methodology, Formal analysis, Writing – original draft, Writing – review & editing. Funding acquisition, Project administration

Declaration of competing interest

The authors have declared that no competing interests exist.

Acknowledgements

The work was financially supported by the Swedish Research Council Formas (2018–01346). The authors would like to thank Dr Friederike Ziegler for help with sourcing raw materials. Professor Paul Knox is gratefully acknowledged for kindly providing monoclonal antibody BAM10. Ana Miljkovic is kindly acknowledged for technical assistance.

Appendix A. Supplementary data

Supplementary data to this article can be found online at https://doi.org/10.1016/j.foodhyd.2021.106989.

References

Abdollahi, M., Axelsson, J., Carlsson, N. G., Nylund, G. M., Albers, E., & Undeland, I. (2019). Effect of stabilization method and freeze/thaw-aided precipitation on structural and functional properties of proteins recovered from brown seaweed (Saccharina latissima). *Food Hydrocolloids, 96*(March), 140–150. https://doi.org/10.1016/j.foodhyd.2019.05.007

Adams, J. M. M., Toop, T. A., Donnison, I. S., & Gallagher, J. A. (2011). Seasonal variation in Laminaria digitata and its impact on biochemical conversion routes to biofuels. Bioresource Technology. https://doi.org/10.1016/j.biortech.2011.08.032.

Allahgholi, L., Sardari, R. R. R., Hakvåg, S., Ara, K. Z. G., Kristjansdottir, T., Aasen, I. M., et al. (2020). Composition analysis and minimal treatments to solubilize polysaccharides from the brown seaweed Laminaria digitata for microbial growth of thermophiles. *Journal of Applied Phycology*. https://doi.org/10.1007/s10811-020-02103-6

Anastasakis, K., Ross, A. B., & Jones, J. M. (2011). Pyrolysis behaviour of the main carbohydrates of brown macro-algae. *Fuel, 90*(2), 598–607. https://doi.org/10.1016/j.fuel.2010.09.023

Appeldoorn, M. M., Kabel, M. A., Van Eylen, D., Gruppen, H., & Schols, H. A. (2010). Characterization of oligomeric xylan structures from corn fiber resistant to pretreatment and simultaneous saccharification and fermentation. *Journal of Agricultural and Food Chemistry*. https://doi.org/10.1021/jf102849x

Bernaerts, T. M. M., Gheysen, L., Foubert, I., Hendrickx, M. E., & Van Loey, A. M. (2019). Evaluating microalgal cell disruption upon ultra high pressure homogenization. *Algal Research*. https://doi.org/10.1016/j.algal.2019.101616

Bradford, M. M. (1976). A rapid and sensitive method for the quantitation of microgram quantities of protein utilizing the principle of protein-dye binding. *Analytical Biochemistry*. https://doi.org/10.1016/0003-2697(76)90527-3

Cofrades, S., López-López, I., Solas, M. T., Bravo, L., & Jiménez-Colmenero, F. (2008). Influence of different types and proportions of added edible seaweeds on characteristics of low-salt gel/emulsion meat systems. *Meat Science, 79*(4), 767–776. https://doi.org/10.1016/j.meatsci.2007.11.010

FAO, Ferdouse, F., Løvstad Holdt, S., Smith, R., Murúa, P., Yang, Z., et al. (2018). The global status of seaweed production, trade and utilization. *FAO Globefish Research Programme, 124*, 120.

Flórez-Fernández, N., Torres, M. D., González-Muñoz, M. J., & Domínguez, H. (2018). Potential of intensification techniques for the extraction and depolymerization of fucoidan. *Algal Research*. https://doi.org/10.1016/j.algal.2018.01.002

World Wildlife Foundation, Foods, K., & Adam, D. (2019). *50 foods for healthier people and a healthier planet* (Vol. 59). Retrieved from https://www.wwf.org.uk/sites/default/files/2019-02/Knorr_Future_50_Report_FINAL_Online.pdf.

Frafinho, P., Raymundo, A., Sousa, I., Dominguez, H., & Torres, M. D. (2019). *Edible Brown Seaweed in Gluten-Free Pasta : Foods, 8*(622), 1–17.

Gomez, L. P., Alvarez, C., Zhao, M., Tiwari, U., Curtin, J., Garcia-Vaquero, M., et al. (2020). Innovative processing strategies and technologies to obtain hydrocolloids from macroalgae for food applications. *Carbohydrate Polymers, 248*(March). https://doi.org/10.1016/j.carbpol.2020.116784

Graiff, A., Ruth, W., Kragl, U., & Karsten, U. (2016). Chemical characterization and quantification of the brown algal storage compound laminarin — a new methodological approach. *Journal of Applied Phycology*. https://doi.org/10.1007/s10811-015-0563-z

Gupta, S., & Abu-Ghannam, N. (2011). Recent developments in the application of seaweeds or seaweed extracts as a means for enhancing the safety and quality attributes of foods. *Innovative Food Science & Emerging Technologies, 12*(4), 600–609. https://doi.org/10.1016/j.ifset.2011.07.004

Herrero, M., Thornton, P. K., Mason-D'Croz, D., Palmer, J., Benton, T. G., Bodirsky, B. L., et al. (2020). Innovation can accelerate the transition towards a sustainable food system. *Nature Food, 1*(5), 266–272. https://doi.org/10.1038/s43016-020-0074-1

Hou, X., Hansen, J. H., & Bjerre, A. B. (2015). Integrated bioethanol and protein production from brown seaweed Laminaria digitata. *Bioresource Technology, 197*, 310–317. https://doi.org/10.1016/j.biortech.2015.08.091

Kumar, S., Gupta, R., Kumar, G., Sahoo, D., & Kuhad, R. C. (2013). Bioethanol production from Gracilaria verrucosa, a red alga, in a biorefinery approach. *Bioresource Technology, 135*, 150–156. https://doi.org/10.1016/j.biortech.2012.10.120

Li, B., Lu, F., Wei, X., & Zhao, R. (2008). Fucoidan: Structure and bioactivity. *Molecules, 13*(8), 1671–1695. https://doi.org/10.3390/molecules13081671

López-López, I., Bastida, S., Ruiz-Capillas, C., Bravo, L., Larrea, M. T., Sánchez-Muniz, F., et al. (2009). Composition and antioxidant capacity of low-salt meat emulsion model systems containing edible seaweeds. *Meat Science, 83*(3), 492–498. https://doi.org/10.1016/j.meatsci.2009.06.031

Lopez-Sanchez, P., Nijsse, J., Blonk, H. C. G., Bialek, L., Schumm, S., & Langton, M. (2011a). Effect of mechanical and thermal treatments on the microstructure and rheological properties of carrot, broccoli and tomato dispersions. *Journal of the Science of Food and Agriculture*. https://doi.org/10.1002/jsfa.4168

Lopez-Sanchez, P., Svelander, C., Bialek, L., Schumm, S., & Langton, M. (2011b). Rheology and microstructure of carrot and tomato emulsions as a result of high-pressure homogenization conditions. *Journal of Food Science, 76*(1). https://doi.org/10.1111/j.1750-3841.2010.01894.x

Lovegrove, A., Edwards, C. H., De Noni, I., Patel, H., El, S. N., Grassby, T., et al. (2017). Role of polysaccharides in food, digestion, and health. *Critical Reviews in Food Science and Nutrition, 57*(2), 237–253. https://doi.org/10.1080/10408398.2014.939263

Lucas, S., Gouin, S., & Lesueur, M. (2019). Seaweed consumption and label preferences in France. *Marine Resource Economics, 34*(2), 143–162. https://doi.org/10.1086/704078

Macosko, C. W. (1994). *Rheology: Principles, measurements, and applications*. Wiley.

Martínez-Abad, A., Giummarella, N., Lawoko, M., & Vilaplana, F. (2018). Differences in extractability under subcritical water reveal interconnected hemicellulose and lignin recalcitrance in birch hardwoods. *Green Chemistry*. https://doi.org/10.1039/c8gc00385h

McKee, L. S., Sunner, H., Anasontzis, G. E., Toriz, G., Gatenholm, P., Bulone, V., et al. (2016). A GH115 α-glucuronidase from Schizophyllum commune contributes to the synergistic enzymatic deconstruction of softwood glucuronoarabinoxylan. *Biotechnology for Biofuels*. https://doi.org/10.1186/s13068-015-0417-6

Moelants, K. R. N., Cardinaels, R., Van Buggenhout, S., Van Loey, A. M., Moldenaers, P., & Hendrickx, M. E. (2014). A review on the relationships between processing, food structure, and rheological properties of plant-tissue-based food suspensions. *Comprehensive Reviews in Food Science and Food Safety, 13*(3), 241–260. https://doi.org/10.1111/1541-4337.12059

Nguyen, T. T., Mikkelsen, M. D., Nguyen Tran, V. H., Dieu Trang, V. T., Rhein-Knudsen, N., Holck, J., et al. (2020). Enzyme-assisted fucoidan extraction from brown macroalgae fucus distichus subsp. Evanescens and saccharina latissima. *Marine Drugs*. https://doi.org/10.3390/md18060296

Palmieri, N., & Forleo, M. B. (2020). The potential of edible seaweed within the western diet. A segmentation of Italian consumers. *International Journal of Gastronomy and Food Science, 20*(February). https://doi.org/10.1016/j.ijgfs.2020.100202

Prabhasankar, P., Ganesan, P., Bhaskar, N., Hirose, A., Stephen, N., Gowda, L. R., et al. (2009). Edible Japanese seaweed, wakame (Undaria pinnatifida) as an ingredient in pasta: Chemical, functional and structural evaluation. *Food Chemistry, 115*(2), 501–508. https://doi.org/10.1016/j.foodchem.2008.12.047

Qin, Y. (2008). Alginate fibres: An overview of the production processes and applications in wound management. *Polymer International, 57*, 171–180. https://doi.org/10.1002/pi.2296

Ruthes, A. C., Martínez-Abad, A., Tan, H. T., Bulone, V., & Vilaplana, F. (2017). Sequential fractionation of feruloylated hemicelluloses and oligosaccharides from wheat bran using subcritical water and xylanolytic enzymes. *Green Chemistry*. https://doi.org/10.1039/c6gc03473j

Saravana, P. S., Cho, Y. N., Woo, H. C., & Chun, B. S. (2018). Green and efficient extraction of polysaccharides from brown seaweed by adding deep eutectic solvent in subcritical water hydrolysis. *Journal of Cleaner Production*. https://doi.org/10.1016/j.jclepro.2018.07.151

Schiener, P., Black, K. D., Stanley, M. S., & Green, D. H. (2014). The seasonal variation in the chemical composition of the kelp species Laminaria digitata, Laminaria hyperborea, Saccharina latissima and Alaria esculenta. *Journal of Applied Phycology*. https://doi.org/10.1007/s10811-014-0327-1

Schultz, S., Wagner, G., Urban, K., & Ulrich, J. (2004). High-pressure homogenization as a process for emulsion formation. *Chemical engineering and technology*. https://doi.org/10.1002/ceat.200406111

Ścieszka, S., & Klewicka, E. (2019). Algae in food: A general review. *Critical Reviews in Food Science and Nutrition, 59*(21), 3538–3547. https://doi.org/10.1080/10408398.2018.1496319

Shi, N., Li, X., Fan, T., Zhou, H., Ding, J., Zhang, D., et al. (2011). Biogenic N-I-codoped TiO2 photocatalyst derived from kelp for efficient dye degradation. *Energy & Environmental Science*. https://doi.org/10.1039/c0ee00363h

Stading, M., & Bohlin, L. (2001). Contraction flow measurements of extensional properties. *Annual Transactions of the Nordic Rheology Society, 8*(9), 181–185.

Wang, H. M. D., Chen, C. C., Huynh, P., & Chang, J. S. (2015). Exploring the potential of using algae in cosmetics. *Bioresource Technology, 184*, 355–362. https://doi.org/10.1016/j.biortech.2014.12.001

Wei, N., Quarterman, J., & Jin, Y. S. (2013). Marine macroalgae: An untapped resource for producing fuels and chemicals. *Trends in Biotechnology, 31*(2), 70–77. https://doi.org/10.1016/j.tibtech.2012.10.009

Wendin, K., & Undeland, I. (2020). Seaweed as food – attitudes and preferences among Swedish consumers. A pilot study. *International Journal of Gastronomy and Food Science*. https://doi.org/10.1016/j.ijgfs.2020.100265

Wikström, K., & Bohlin, L. (1999). Extensional flow studies of wheat flour dough. I. Experimental method for measurements in contraction flow geometry and application to flours varying in breadmaking performance. *Journal of Cereal Science*. https://doi.org/10.1006/jcrs.1999.0251

Yilmaz-Turan, S., Jiménez-Quero, A., Moriana, R., Arte, E., Katina, K., & Vilaplana, F. (2020). Cascade extraction of proteins and feruloylated arabinoxylans from wheat bran. *Food Chemistry*. https://doi.org/10.1016/j.foodchem.2020.127491

Zhou, L., Guan, Y., Bi, J., Liu, X., Yi, J., Chen, Q., et al. (2017). Change of the rheological properties of mango juice by high pressure homogenization. *Lebensmittel-Wissenschaft & Technologie, 82*, 121–130. https://doi.org/10.1016/j.lwt.2017.04.038

Zvyagintseva, T. N., Shevchenko, N. M., Popivnich, I. B., Isakov, V. V., Scobun, A. S., Sundukova, E. V., et al. (1999). A new procedure for the separation of water-soluble polysaccharides from brown seaweeds. *Carbohydrate Research*. https://doi.org/10.1016/S0008-6215(99)00206-2